

# Substitution of Thiophene Oligomers with Macrocyclic End Caps and the Colorimetric Detection of Hg(II)

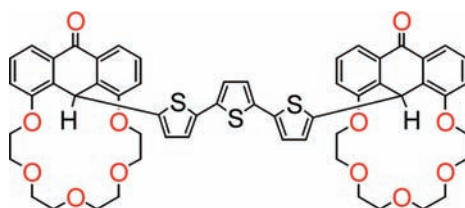
Mariappan Kadarkaraisamy, Soudsakhone Thammavongkeo, Prem N. Basa, Gerald Caple, and Andrew G. Sykes\*

Department of Chemistry, University of South Dakota, Vermillion, South Dakota 57069, United States

asykes@usd.edu

Received March 8, 2011

## ABSTRACT



Alkyl substitution at the  $\alpha$  position(s) of mono-, bi-, and terthiophenes via electrophilic addition of macrocyclic end caps combines linear,  $\pi$ -conjugated aromatic compounds and annular macrocycles. Addition of the Hg(II) ion to terthiophene adducts produces intense color changes, allowing for the selective, colorimetric detection of mercury(II). Chemical oxidation of the asymmetric terthiophene adduct produces the sexithiophene oligomer.

Several articles have recently described the importance of linear  $\pi$ -conjugated oligomers and polymers that have been synthesized for use in energy and sensor related applications.<sup>1,2</sup> The vast majority of substitution chemistry that is undertaken on linear  $\pi$ -conjugated systems involves metalation reactions of primarily halo-substituted aromatic heterocycles.<sup>3</sup> Examples include mercuration,<sup>4</sup> lithiation,<sup>5</sup> Stille coupling (Sn),<sup>6</sup> and Suzuki coupling (Pd)<sup>7</sup> of heteroaromatic compounds and associated oligomeric starting materials. Electrophilic addition involving

aromatic heterocycles (below) has received considerable less attention than above, even though simple common furans, thiophenes, and pyrroles are produced this way (i.e., via nitration or sulfonation for example), and the growth of polythiophene or polypyrrole, either chemically or electrochemically, essentially occurs by this same mechanism.



(1) (a) Cheng, Y. T.; Yang, S. A.; Hsu, C. S. *Chem. Rev.* **2009**, *109*, 5868. (b) Gunes, S.; Neugebauer, H.; Sariciftei, N. S. *Chem. Rev.* **2007**, *107*, 1324. (c) McQuade, M. T.; Pullen, A. E.; Swager, T. M. *Chem. Rev.* **2000**, *100*, 2537. (d) Roncali, J. *Chem. Rev.* **1997**, *97*, 173. (e) Roncali, J. *Chem. Rev.* **1992**, *92*, 711.

(2) (a) Huss, A. S.; Rossini, J. E.; Ceckanowicz, D. J.; Bohnsack, J. N.; Mann, K. R.; Gladfelter, W. L.; Blank, D. A. *J. Phys. Chem. C* **2011**, *115*, 2 and references therein.

(3) Handbook of Thiophene-based Materials Vol. 1: *Synthesis and Materials*; Perepichka, I. E., Perepichka, D. F., Eds.; Wiley: U.K. 2009.

(4) (a) Buzhansky, L.; Feit, B. A. *J. Org. Chem.* **2002**, *67*, 7523. (b) Hoffa, S.; Lee, S. A.; Tamaki, T. *J. Heterocycl. Chem.* **2000**, *37*, 25.

(5) Marino, G. *Adv. Heterocycl. Chem.* **1971**, *13*, 235.

(6) Hei, J.; Cho, W.; Jin, S. H.; Yoon, U. C. *Bull. Korean Chem. Soc.* **2007**, *28*, 7.

(7) (a) Melucci, M.; Barbarella, G.; Zambianchi, M.; Di Petro, P.; Bongini, A. *J. Org. Chem.* **2004**, *69*, 4821. (b) Tsigvoulis, G. M.; Lehn, J. M. *Adv. Mater.* **1997**, *9*, 39.

We have previously demonstrated the reaction of nitriles with compound **1** (Scheme 1) that produces secondary amides in the presence of an acid catalyst.<sup>8</sup> The amide carbonyl is itself protonated and forms an intraannular hydrogen bond where, upon deprotonation, a large amplitude change in geometry occurs that leaves the macrocyclic pore unblocked. The production of amides from nitriles was originally discovered by Ritter,<sup>9</sup> where

(8) Kadarkaraisamy, M.; Caple, G.; Gorden, A. R.; Sykes, A. G. *Inorg. Chem.* **2008**, *47*, 11644.

(9) (a) Ritter, R.; Minieri, P. P. *J. Am. Chem. Soc.* **1948**, *70*, 4045–48. (b) The Ritter Reaction: Krimin, L.I.; Cota, D.J., *Organic Reactions*; Kriger Publishing: 1969; pp 213–325.

### Scheme 1



protonation of the secondary alcohol produces a better leaving group in water, resulting in the formation of a carbocation intermediate that reacts with nucleophiles present in solution. Additional investigations have led us to the addition of compounds that contain other types of nucleophiles such as imines and primary amides as well.<sup>10</sup>

This investigation focuses on the alkylation of activated heterocyclic ring compounds (thiophenes), and this chemistry has been extended to bi- and terthiophene oligomers for the first time, producing symmetric and asymmetric substituted  $\pi$ -conjugated heteroaromatics containing macrocyclic end caps. Electrophilic addition of thiophene and pyrrole subunits with secondary alcohols has very recently been employed to create novel porphyrinoid type mimics.<sup>11</sup> Described within is the synthesis, X-ray crystallography, electrochemistry, and spectroscopy of new  $\pi$ -conjugated oligomers capped with annular macrocycles, along with their optical sensing properties in the presence of Hg(II) ion.

The addition of simple nitriles to **1** in the presence of perchloric acid has previously been shown to produce secondary amides in good yield.<sup>8</sup> When 3-thiopheneacetonitrile is substituted instead, which contains two potential nucleophiles—the nitrile and the activated aromatic thiophene ring—which has the possibility of a competition reaction, only the  $\alpha$ -substituted heterocyclic ring product was produced. The X-ray crystal structure of **2** is shown in Figure 1. Substitution at the  $\alpha$  position of the thiophene ring is readily apparent as opposed to the formation of an amide if the cyano group acted as the nucleophile. The thiophene ring also reacts at the 2-position, as opposed to the 5-position, which is also confirmed by a pair of doublets with a 5.2 Hz coupling constant for the two adjacent thiophene protons in the <sup>1</sup>H NMR spectra of **2**. The thiophene is also rotated such that the methylene group on the thiophene sits adjacent to the empty and less sterically crowded polyether ring. Crystallographic data for all structures are provided in Table S1.

Compounds **3** thru **6** which introduce bithiophene and terthiophene oligomers as nucleophiles undergo identical substitution under the same reaction conditions. Reactions

(10) Kadarkaraisamy, M.; Gable, G.; Basa, P. N.; Sykes, A. G. *Tetrahedron* **2011**, submitted.

(11) (a) Stepien, M.; Szyszko, B.; Latos-Grazynski, L. *Org. Lett.* **2009**, *11*, 3930. (b) Zhang, Z.; Ferrence, G. M.; Lash, T. D. *Org. Lett.* **2009**, *11*, 101. (c) Reddy, J. S.; Anand, V. G. *Chem. Commun.* **2008**, 1326.

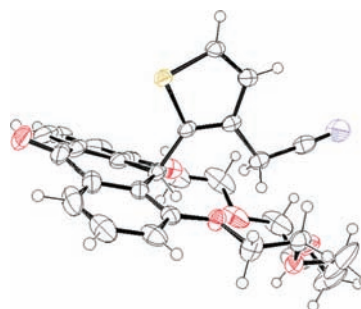


**Figure 1.** Thermal ellipsoid diagram (30%) of the (3-acetonitrile)thiophene anthracenone adduct (**2**).

of equal molar amounts of the anthracenone **1** and bithiophene or terthiophene produce 1:1 adducts (compounds **3** and **5**), while reaction using a 2-fold excess of **1** produces symmetric products where both available  $\alpha$  positions have been substituted with anthracenone end caps (compounds **4** and **6**). The <sup>1</sup>H NMR spectra for compounds **3–6** have in common two doublets and a triplet in the aromatic region attributed to the symmetric 1,8-disubstituted anthracenone moiety (~7.8, 7.4, and 7.0 ppm); multiplets from 3.8 to 4.6 ppm due to the CH<sub>2</sub>–O protons of the polyether chain; and a sharp singlet at ~6.3 ppm for the anthracenone methine proton. Compound **3**, the bithiophene monomer, shows multiplets equivalent to five protons from 6.79 to 6.91 ppm for the bithiophene. Compound **4** shows two simple doublets at 6.56 and 6.88 with 4.0 Hz coupling constants for the symmetrically disubstituted bithiophene. Compound **5** has multiplets equivalent to seven protons from 6.81 to 6.91 ppm for the asymmetric substituted terthiophene, and compound **6** shows a singlet at 6.70 and two doublets at 6.73 and 6.89 with 4.0 Hz coupling constants characteristic of a symmetric disubstituted terthiophene. The proton NMR spectra of the aromatic region for compounds **3–6** are provided in Figures S1–S4 in the Supporting Information.

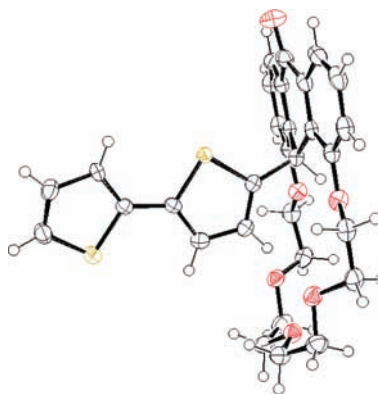


**Figure 2.** Thermal ellipsoid diagram (30%) of the bithiophene monomer (**3**).

In addition we have structurally characterized three of the above four compounds. The thermal ellipsoid diagrams for compounds **3** through **5** are given in Figures 2 through 4. The 1:1 and 1:2 bithiophene adducts, **3** and **4**, clearly show the staggered configuration of the bithiophene linker in the solid state. In the case of **4**, the molecule has pseudo  $C_2$  symmetry and both thiophenes are oriented such that the hydrogen atoms on the thiophene  $\beta$  positions point into the empty ring instead of toward the anthracenone (Figure 3). The least-squares planes for the two

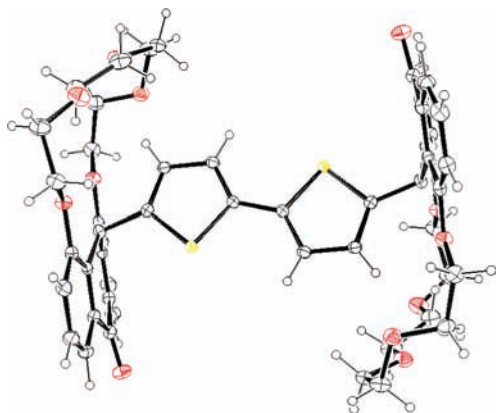


**Figure 3.** Thermal ellipsoid diagram (30%) of the bithiophene dimer (**4**).

thiophene rings in **3** have a dihedral angle of  $13.6^\circ$ , while the two thiophene rings are perfectly coplanar (centrosymmetric) in **4**. We have only been able to grow crystals of the terthiophene 1:1 adduct, **5**, the structure of which is provided in Figure 4. In this structure, the terminal thiophene ring is found disordered in two opposite configurations over two positions in a 2:1 ratio. For the larger occupancy, the sulfur atoms adopt an *anti* configuration compared to the middle thiophene, while the middle thiophene is itself *syn* to the thiophene ring bonded

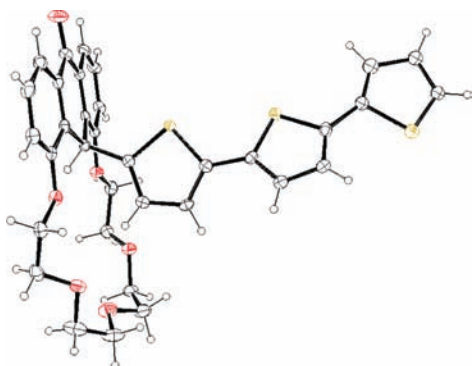


**Figure 4.** Thermal ellipsoid diagram (30%) of the terthiophene monomer (**5**). Only the larger occupancy of the terminal thiophene (67%) is shown.

**Table 1.** Cyclic Voltammetric Data (V); 0.05 M TBAH/ $\text{CH}_2\text{Cl}_2$  vs Ag/AgCl on Glassy Carbon

compd	$E_{a1}$	$E_{a2}$	$E_{a3}$	$E_c$	$E^\circ$
<b>3</b>	1.09	1.47	–	0.25	–1.70
<b>4</b>	1.12	1.53	–	weak	–1.71
<b>5</b>	1.08	1.20	1.61	0.17	–1.76
<b>6</b>	0.90	1.15	1.53	weak	–1.71

to the anthracenone. The outer two rings have a dihedral angle of  $20.6^\circ$  (for the larger occupancy), while the inner two rings represent the largest deviation from planarity with a dihedral angle of  $33.0^\circ$ .

Cyclic voltammetry data for compounds **3**–**6** are listed in Table 1. Electrochemistry reveals there are two irreversible oxidation peaks for the bithiophene adducts, representing successive oxidation of the two thiophene aromatic rings. Compound **3** leaves the outer thiophene ring unsubstituted in the  $\alpha$ -position allowing for the potential coupling of monomers upon electrochemical oxidation; however no increase in peak currents characteristic of conducting film formation was observed with repeated cycling. For the terthiophene adducts, **5** and **6**, three irreversible oxidation waves are observed instead of two for the bithiophene adducts. Repeated cycling to 1.5 V for the monosubstituted terthiophene adduct with only a single end cap, **5**, does produce growth in peak currents characteristic of the growth of a conducting polymer film on the surface of the glassy carbon electrode (Figure S5).

Adducts with two end caps, compounds **4** and **6**, only have a weak return oxidation after cycling to 1.5 V, whereas compounds **3** and **5** (single end-cap) have significant return reductions at  $\sim 0.2$  V. In addition, all four of these compounds have reversible reduction peaks at  $\sim -1.7$  V due to reduction of the single anthracenone carbonyl group.

We also tested compounds **3**–**6** against a battery of different metals ( $\text{Li}^+$ ,  $\text{Na}^+$ ,  $\text{Mg}^{2+}$ ,  $\text{Ca}^{2+}$ ,  $\text{Sr}^{2+}$ ,  $\text{Mn}^{2+}$ ,  $\text{Co}^{2+}$ ,  $\text{Ni}^{2+}$ ,  $\text{Zn}^{2+}$ ,  $\text{Cd}^{2+}$ ,  $\text{Hg}^{2+}$ , and  $\text{Pb}^{2+}$ ) to determine if these compounds have the ability to act as metal ion sensors. The only metal that produced any change in the absorption spectrum was the mercury(II) ion (Figure 5).

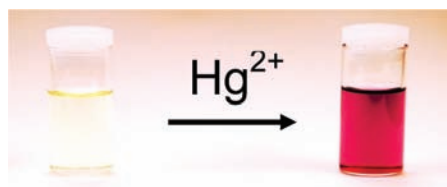


**Figure 5.** Visual changes with addition of  $\text{Hg}(\text{II})$  to **5**.

The UV–vis spectra for both terthiophene substituted anthracenones, compounds **5** and **6**, show the formation of intense absorption bands at 532 nm after the addition of

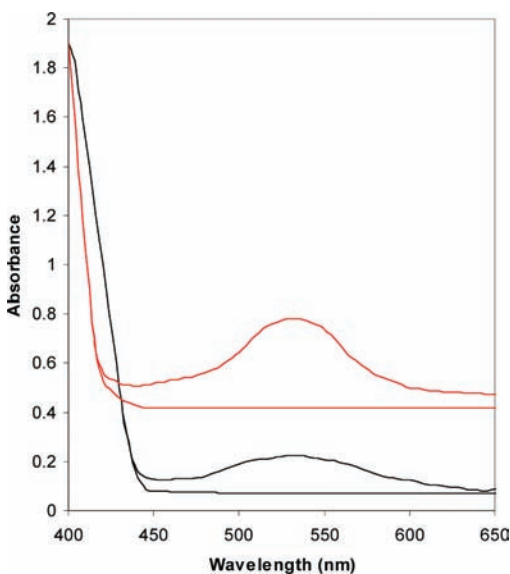


**Figure 6.** UV/vis spectra of **5** (red) and **6** ( $1.0 \times 10^{-4}$  M) before and after addition of 2.0 equiv of  $\text{Hg}(\text{ClO}_4)_2$  in dichloromethane. The spectra of **5** (red) have been offset for clarity.

$\text{Hg}(\text{ClO}_4)_2$  in dichloromethane, Figure 6. No color change is observed upon the addition of mercury(I) salts. The bithiophene substituted compounds, **3** and **4**, do not produce any color change in the presence of  $\text{Hg}(\text{II})$  either. We attribute the new absorption band to the interaction of the sulfurphilic  $\text{Hg}(\text{II})$  ion with the sulfur atoms of the terthiophene unit and the formation of a charge transfer band due to partial oxidation of the terthiophene unit ( $\epsilon = \sim 3000 \text{ M}^{-1} \text{ cm}^{-1}$ ). This is a simple sensing mechanism for mercury and decidedly different from other numerous Photoinduced Electron Transfer (PET) sensors which couple a selective receptor to a fluorophore. The red color

gradually fades with concomitant formation of a dark green/black solid after several hours. Addition of only 0.5 equiv of  $\text{Hg}(\text{II})$  maintains the color change for a significantly longer period of time. Addition of 1 equiv of the stronger chemical oxidants  $\text{Fe}(\text{III})$  or  $\text{Cu}(\text{II})$  to **5** in dichloromethane immediately produces a dark green/black solid that we attribute to the formation of a sexithiophene oligomer symmetrically substituted with two anthracenone end caps, i.e.  $\text{C}_{22}\text{H}_{23}\text{O}_6-(\text{C}_4\text{H}_2\text{S})_6-\text{C}_{22}\text{H}_{23}\text{O}_6$ . After filtering and washing with diethyl ether, this product is moderately soluble in  $\text{CDCl}_3$  and still shows the presence of the methine protons at 6.35 ppm. The polyether methylene protons are in correct proportion to the number of methine, aromatic anthracenone and thiophene protons (Figure S6) expected for formation of a symmetrically substituted sexithiophene adduct. Mass spectral data for the sexithiophene parent ion and MS-MS fragments are provided in the Supporting Information and only a broad shift in absorbance to the red is observed indicating lengthened conjugation and no additional oxidation has occurred. Attempts to crystallize the end-capped sexithiophene product and the mercury/terthiophene adduct are ongoing at this time.

**Acknowledgment.** The authors thank NSF-EPSCOR (EPS-0554609) and the South Dakota Governor's 2010 Initiative for financial support and the purchase of a Bruker SMART APEX II CCD diffractometer. The elemental analyzer was provided by funding from NSF-URC (CHE-0532242). S.T. and P.N.B. thank the University of South Dakota and NSF-EPSCoR (EPS-0903804) for financial support.

**Supporting Information Available.** Experimental procedures, crystallographic data, and full spectroscopic data for all new compounds. This material is available free of charge via the Internet at <http://pubs.acs.org>.